

Article

Advanced Adaptive Rule-Based Energy Management for Hybrid Energy Storage Systems (HESSs) to Enhance the Driving Range of Electric Vehicles

Chew Kuew Wai ^{1,*} , Taha Sadeq ^{2,*}  and Lee Cheun Hau ¹ 

¹ Lee Kong Chian Faculty of Engineering and Science, Universiti Tunku Abdul Rahma, Sungai Long Campus, Kajang 43000, Selangor, Malaysia; haulc@utar.edu.my

² Faculty of Mechanical and Manufacturing Engineering, Universiti Tun Hussein Onn Malaysia, Parit Raja Campus, Parit Raja 86400, Johor, Malaysia

* Correspondence: chewkw@utar.edu.my (C.K.W.); tmahmed@uthm.edu.my (T.S.)

Abstract: The energy storage system (ESS) plays a crucial role in electric vehicles (EVs), impacting their performance and efficiency. While batteries are the standard choice for energy storage, they come with drawbacks like low power density and limited life cycles, which can hinder pure battery electric vehicles (PBEVs). To address these issues, a hybrid energy storage system (HESS) that combines a battery with a supercapacitor provides a more effective solution. The battery delivers consistent power, while the supercapacitor manages peak power demands and regenerative braking energy. This study proposes a new energy management strategy for the HESS, an advanced adaptive rule-based algorithm. The results of the standard rule-based and adaptive rule-based algorithms are used to verify the proposed control algorithm. The system was modeled in MATLAB/Simulink and evaluated across three driving cycles—UDDS, NYCC, and Japan1015—while varying states of charge for the supercapacitors. The findings indicate that the HESS significantly alleviates battery stress compared to a pure battery system, enhancing both efficiency and lifespan. Among the algorithms tested, the advanced adaptive rule-based algorithm yielded the best results, increasing the number of viable drive cycles.

Keywords: batteries; supercapacitors; adaptive algorithm; hybrid energy storage; electric vehicle



Academic Editor: Adolfo Dannier

Received: 13 October 2024

Revised: 23 December 2024

Accepted: 15 January 2025

Published: 18 January 2025

Citation: Wai, C.K.; Sadeq, T.; Hau, L.C. Advanced Adaptive Rule-Based Energy Management for Hybrid Energy Storage Systems (HESSs) to Enhance the Driving Range of Electric Vehicles. *Vehicles* **2025**, *7*, 6. <https://doi.org/10.3390/vehicles7010006>

Copyright: © 2025 by the authors. Licensee MDPI, Basel, Switzerland. This article is an open access article distributed under the terms and conditions of the Creative Commons Attribution (CC BY) license (<https://creativecommons.org/licenses/by/4.0/>).

1. Introduction

The growing interest in the energy storage system (ESS) stems from the need to shift from fossil fuels to renewable resources for energy production, driven by two awarenesses: the eventual depletion of petroleum reserves and the issue of global warming. This shift has led to a significant increase in the number of electric vehicles (EVs) on the market, due to advancements in power electronic converters, their eco-friendliness, and the ability to regenerate energy through braking. EVs are more efficient than conventional vehicles, require less maintenance due to fewer moving parts, and have a significant impact on reducing air pollution. Since the 1970s, the amount of emissions produced worldwide by burning fossil fuels has grown by 90% and, in 2014, emissions reached an all-time high of approximately 36.1 Gt. A national goal in certain nations is now lowering CO₂ emissions. Canada, for instance, wants to reduce its greenhouse gas emissions from 2007 levels by 33 percent by 2020 and 80 percent by 2050. The transportation industry is one of the biggest producers of greenhouse gases. The consumption of fossil fuels by internal combustion engine (ICE) cars is the primary cause of 82.5 percent of transportation emissions in Canada, which come from road transportation [1].

Although batteries are the most common energy storage systems (ESSs) and show significant potential for supporting clean energy [2], studies indicate that a single electric system cannot yet match the performance of internal combustion engines [3–6]. Consequently, considerable research has focused on improving battery cells for electric vehicle (EV) applications. Lead–acid batteries account for 40–45% of global battery sales due to their availability, reliability, and affordability [7]. Meanwhile, lithium-ion batteries are widely used in battery electric vehicles (BEVs) for their superior specific energy and power densities. Research suggests that BEVs require batteries with a specific energy of approximately 0.235 kWh/kg and a specific power of around 0.470 kW/kg to meet performance targets. To cover a distance of 500 km, around 100 kg of lithium-ion batteries would be needed, providing energy comparable to a full tank of gasoline. Additionally, studies show that EV drivers travel an average of 20,000 km annually, using roughly 2.7 kWh for every 50 km driven, highlighting the efficiency and suitability of lithium-ion batteries for long-distance EV use [8,9].

The electric vehicle industry continues to face several challenges that demand the attention of researchers and industry experts [5,10,11]. One of the key limitations of battery electric vehicles (BEVs) is their limited life cycle and low power density. A promising solution to these challenges is the adoption of a hybrid energy storage system for EV applications [12–14]. A HESS integrates two or more types of energy storage devices, such as batteries, fuel cells, flywheels, or supercapacitors, to enhance energy delivery performance. In this system, a primary energy storage device, like a battery or fuel cell with high energy density, provides a steady power supply to the load, while an auxiliary device, such as a supercapacitor or flywheel with high power density, responds rapidly to sudden changes in power demand. This synergy allows the HESS to efficiently handle both continuous energy needs and dynamic load fluctuations, improving the overall performance and longevity of the system [15,16].

The HESS faces two primary challenges: selecting the appropriate topology and developing an efficient energy management system (EMS). The EMS plays a critical role in controlling the power flow between the HESS and the load, which directly impacts system performance. Various control strategies, such as optimization-based and rule-based methods, are employed to manage power distribution. The main goal of the EMS is to improve the performance, efficiency, and lifespan of the HESS by ensuring smooth and effective power flow management. However, implementing optimized control strategies can be computationally intensive, presenting challenges in executing the EMS in real time on a standalone embedded system.

Numerous studies have explored different topologies for battery–supercapacitor hybrid systems in electric vehicles [17–20]. Figure 1 illustrates various HESS topologies [21]. The simplest configuration, shown in Figure 1a, involves a direct connection between the battery and supercapacitor, with a DC-DC converter managing power flow. However, this setup restricts the supercapacitor’s performance and requires a full-sized DC-DC converter to handle energy distribution [22,23]. The topology in Figure 1b improves safety by ensuring that battery power remains within a safe operating range using a DC-DC converter, while the supercapacitor acts as an energy buffer with a limited operational range [19]. Figure 1c presents a widely adopted topology [24,25] where a DC-DC converter is employed to interface the supercapacitor with the DC bus, enabling precise control of power flow. This configuration allows the supercapacitor to operate across a broad voltage range, which enhances overall system efficiency by reducing the load on the battery and minimizing battery current. Additionally, this topology improves system reliability, ensuring uninterrupted power flow even in the event of a DC-DC converter failure. Two separate DC-DC converters, shown in Figure 1d,e, are utilized to regulate power flow from

the battery and the supercapacitor independently [26,27]. The arrangement in Figure 1f is subjected to the same limitations as the type in Figure 1d,e, where batteries and supercapacitors are connected in parallel via two DC-DC converters separately. This configuration is called the active HESS.

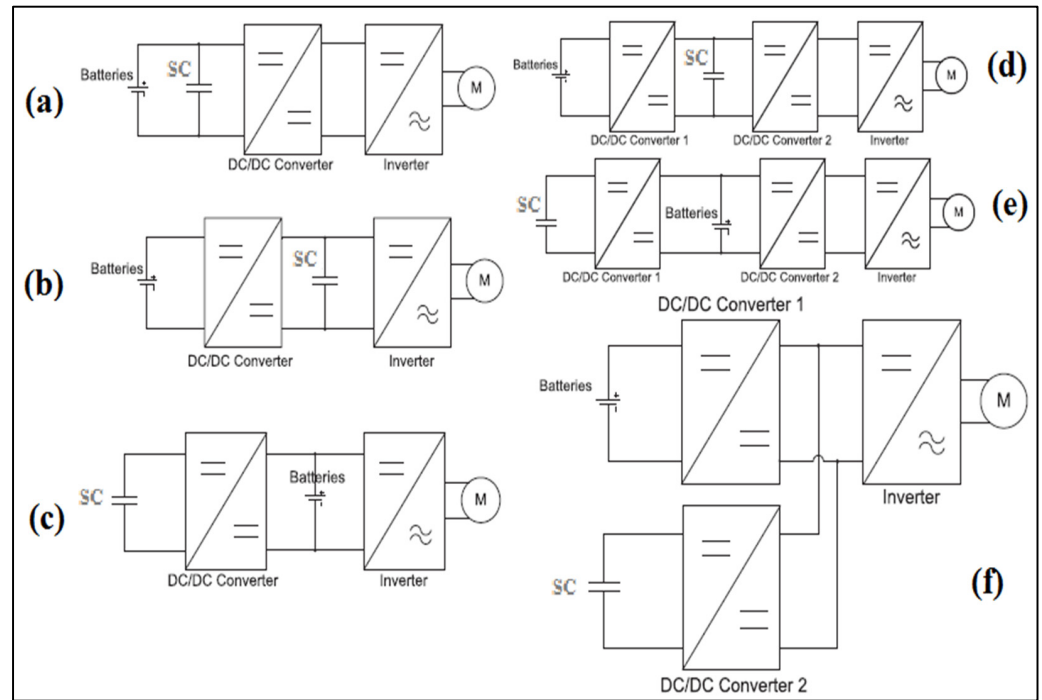


Figure 1. The main topologies for the HESS in the literature. (a) passive topology, (b) semi-active topology type 1, (c) semi-active topology type 2, (d) active topology type 1, (e) active topology type 2, (f) active topology type 3.

The energy management system is essential in active and semi-active topologies of hybrid energy storage systems. Its main function is to distribute power between the battery and supercapacitor, optimizing the overall performance of the HESS. EMS strategies for electric vehicles (EVs) can be generally divided into three categories: optimization-based, rule-based, and pattern-recognition approaches. Extensive research has outlined the unique characteristics of each strategy. Figure 2 illustrates an overview of the main categories of energy management systems.

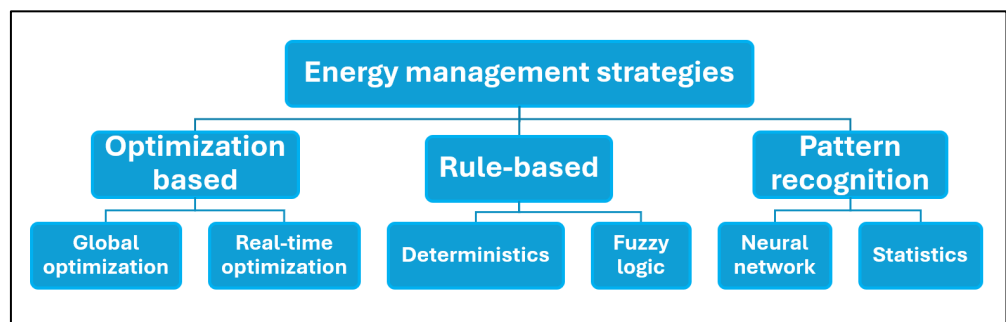


Figure 2. The classification of energy management systems for HESSs.

To maximize the benefits of combining multiple energy sources and enhance the life cycle and system efficiency of electric vehicles, it is crucial to employ a suitable topology for the HESS [28,29]. EV batteries typically have a lifespan from approximately 8 to 10 years, determined by the loss in battery capacity compared to the initial capacity. An appropriate

range for the percentage deterioration is generally considered to be between twenty and thirty percent [30,31]. SOC functions mainly establish the power battery model. The state of charge of the battery is determined by battery capacitance, the initial SOC value, and battery current, which is used to identify the open circuit voltage and resistance value [32].

Two cascaded fuzzy logic controllers and model predictive control (MPC) are proposed to regulate induction motor speed and minimize state of health (SOH) degradation and the reduction of state of charge (SOC) for lithium-ion (Li-ion) batteries. The battery information was used to tune the parameters of the MPC, where a fuzzy logic controller was used to modify the MPC objective function. NEDC and US06 drive cycles were implemented to validate the proposed controllers [33]. The fuzzy logic controller is proposed for the HESS in [34], and the simulation results using Siemens Simcenter Flomaster and ADVISOR programs in the New European Driving Cycle (NEDC) show that the HESS is effective, reducing battery currents by approximately 29%, reducing battery heat generation by 46.84%, and minimizing capacity loss. The system also improves driving range by 3.4% and lowers average energy consumption by 20.43%. An advanced adaptive controller and a fuzzy adaptive controller were developed to manage the energy distribution between the battery and the supercapacitor. The algorithms were tested on three real-world driving cycles—uphill, downhill, and city tour—at three different speeds, 50 km/h, 60 km/h, and 70 km/h, to assess their performance. A new strategy integrates advanced fuzzy logic to optimize braking force distribution under varying conditions for EVs [35]. This approach contributes to sustainable electric vehicle performance and increased vehicle mileage.

A hybrid energy storage system with different batteries and supercapacitors for electric buses is investigated in [36]. In addition to the prior comparison, an economic analysis is conducted from the perspective of life cycle costs. According to the conclusion, the option containing the (SCs/AGM batteries) is the best in terms of cost and is followed by SCs and lithium-ion batteries. The control algorithms for the HESS proposed in [37] incorporate the road slope during the driving journey to optimize the driving range of electric vehicles. A meta rule-based energy management strategy (EMS) for hybrid electric vehicles is presented in [38]. It is intended to enhance battery performance and energy efficiency without depending on predetermined driving patterns. Clustering and feature selection based on mutual information is used to calculate the parameters of the ideal energy management rule, which is represented as a segmented folding line by assessing the outcomes of dynamic programming. The meta rule-based EMS exhibits great computational efficiency appropriate for real-time applications and drastically lowers Li-ion battery Ampere-hour throughput (up to 17% and 16.6%, respectively) in comparison to DPR-based and LSTM-based EMSs.

Proportional integral (PI), model predictive control (MPC), and radial basis function (RBF) controllers were tested for the HESS in [39]. The results demonstrate significant improvements in energy efficiency, battery state of charge (SOC) management, and system responsiveness, with the radial basis function (RBF) controller outperforming traditional methods, particularly in dynamic and unpredictable conditions. The rule-based control strategy is proposed to control energy flow and limit the power drawn from the battery in the HESS of the EV. The fuzzy logic controllers are used alongside the rule-based strategy to enhance the performance of the hybrid energy storage system and promote more efficient energy usage in electric vehicles [40]. Additionally, the investigation explores rule-based active power-sharing strategies in the HESS, where various methods were tried to maximize power distribution between the battery and ultracapacitor according to load fluctuations, peak load requirements, and state of charge (SOC). The results proved that the HESS approach reduces battery stress while offering effective control that enhances system stability and energy management [41]. Lastly, the adaptive rule-based energy management

method is proposed to maximize the performance of the HESS [42]. According to the results of the proposed approach, the HESS can decrease the average output power changing rate of the battery by up to 76.5%, and it can also significantly reduce the average battery current in both the propelling and regeneration modes.

2. System Structure and Modeling

In the literature, previous research on energy management systems for hybrid energy storage systems in electric vehicles has often neglected the importance of regenerative energy during deceleration in the driving cycle [43]. Neglecting this factor may lead to the inability to absorb the regenerative energy during vehicle deceleration by the supercapacitor, if the state of charge of the supercapacitor is at the maximum level. This study aims to fill this gap by proposing an intelligent energy management system tailored for HESSs in EVs, enabling the continuous capture of regenerative energy. The proposed EMS actively estimates the amount of regenerative energy produced throughout the driving cycle and modifies the control algorithm as needed. By optimizing the supercapacitor's use to meet the vehicle's load current, the system keeps the state of charge below the maximum limit, ensuring there is enough capacity to store regenerative energy. This smart control strategy promotes efficient energy recovery during deceleration, enhancing the advantages of the regenerative braking system.

2.1. Hybrid Energy Storage System Model

This study utilizes a semi-active topology for hybrid energy storage systems to meet the energy demands of electric vehicles (EVs). An energy management system is proposed to optimally distribute energy between the battery and supercapacitor, effectively limiting battery current. The supercapacitor stores regenerative energy during braking and provides the peak current required by the EV, while the battery supplies power during low traction and steady-state operation. The control algorithm adjusts the duty cycle of the DC-DC converter to regulate the energy flow from the supercapacitor. Figure 3 illustrates the HESS architecture for the EV used in this study.

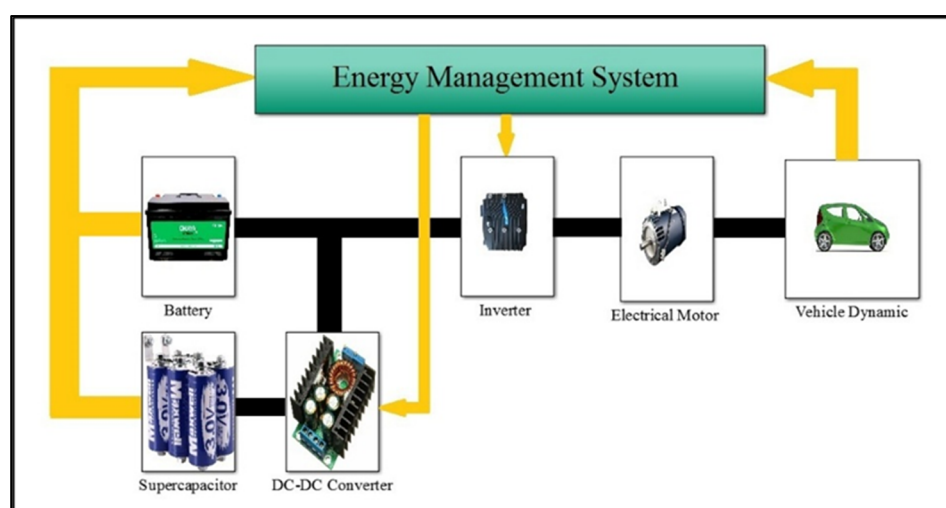


Figure 3. Architecture of HESS for the electric vehicle in this research.

Tables 1 and 2 show the main parameters of the battery model and capacitor used in the current research.

Table 1. Battery model parameters.

Parameter	Value
Capacity	100 Ah
Nominal voltage	500 V
Internal resistance	0.125 Ohm
Stored energy	50 kWh
Initial $B_{SOC}(0)$	0.95

Table 2. Supercapacitor model parameters.

Parameter	Value
Rated voltage	300 V
Resistance	2.1 mΩ
Rated capacitance	100 F
Initial $SC_{soc}(0)$	0.92, 0.51, 0.20

2.2. Electric Vehicle Model

To achieve lower energy usage, an accurate model of EV performance is necessary. While some researchers have utilized ADVISOR to do thorough performance assessments for a variety of vehicles, others have used MATLAB/Simulink to construct the EV model [4,44–48]. A thorough explanation of the vehicle dynamic system is presented in [10,49,50]. Table 3 shows the primary parameters of the EV model; the completed model of the EV’s HESS using MATLAB/Simulink is shown in Figure 4 [28,37,51]. The energy consumption of an electric vehicle is intricately linked to its operating speed due to several factors that influence overall efficiency. At higher speeds, the aerodynamic drag increases exponentially, requiring the vehicle’s motor to work harder to overcome this resistance [52]. Furthermore, an accurate model of the DC-DC converter in an EV is essential because it governs the conversion of electrical power between the battery, motor, and auxiliary systems [53].

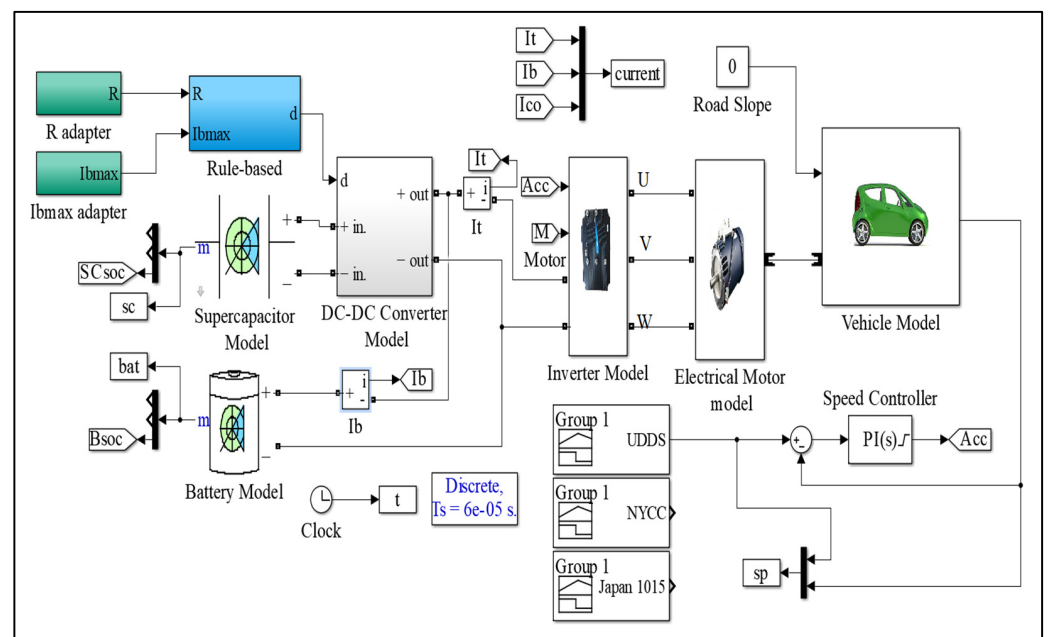


Figure 4. HESS MATLAB/Simulink model based on the standard drive cycles.

Table 3. Electric vehicle model parameters.

Parameter	Value
Vehicle mass (M_v)	1325 kg
Frontal area (A_f)	2.57 m ²
Drag coefficient (C_d)	0.26
Wheel radius	0.3 m
Gravity acceleration (g)	9.8 ms ⁻²
Rolling resistance (μ_{rr})	0.0048
Air density (ρ)	1.29 kg·m ⁻³

3. Designing the Energy Management System of the HESS

Designing a hybrid energy storage system that combines batteries and supercapacitors for electric vehicles poses a significant challenge in real-time energy demand allocation between the primary and auxiliary storage devices. This study investigates a semi-active hybrid energy storage system configuration tailored for EV applications. In real-time control situations, energy management systems typically prefer rule-based strategies over optimization methods, primarily because the optimization process requires a significant amount of computation time. The proposed advanced adaptive rule-based control algorithm presents a practical and efficient solution for managing energy in hybrid energy storage systems in real-time.

Three different rule-based algorithms were tested in this research: a standard rule-based algorithm, an adaptive rule-based algorithm, and an advanced adaptive rule-based algorithm. These algorithms were tested in various states of supercapacitor charge to validate the proposed control algorithms of the HESS in different situations. In the first case, the initial state of charge (SOC) for the supercapacitors was high, at 92%; in the second case, it was moderate, at 51%; and in the third case, it was low, at 20%. The selection of specific drive cycles for testing in automotive and emissions research is crucial to ensure that the results represent real-world driving conditions. In this research, the drive cycles selected are the Urban Dynamometer Driving Schedule (UDDS), the New York City Cycle (NYCC), and the Japan 10-15 Mode Cycle (Japan1015). These drive cycles are commonly used and well recognized for several reasons, including ensuring geographic diversity, which is essential because driving patterns, road infrastructure, and emissions regulations can vary significantly between regions.

3.1. The Standard Rule-Based Algorithm of the HESS

The hybrid energy storage system in [51] was developed to manage power flow using two approaches based on a Rule-Based Linear Quadratic Regulator. Typically, the battery is responsible for meeting low load demands, while supercapacitors are employed to address high load demands. The HESS for electric vehicles was simulated using MATLAB/Simulink. The effectiveness of the algorithms was assessed across three standard driving cycles: the Urban Dynamometer Driving Schedule (UDDS), the New York City Cycle (NYCC), and the Japan1015 driving cycle.

Instantaneous allocation of the HESS current for various drive cycles is achieved through the standard rule-based algorithm. The algorithm is designed to maintain the battery current ($I_b(t)$) at a specified target value (I_{b_max}) while effectively distributing the vehicle load current between the battery and supercapacitor throughout any driving cycle. It manages the energy flow within the hybrid energy storage system across various operational scenarios by taking into account the total demand load current ($I_t(t)$), the state

of charge of the supercapacitor (SOC_{sc}), and the direction of energy flow. The operational parameters of the algorithm are defined as per Equation (1)

$$\begin{cases} \text{If } (I_t > 0) \text{ and } (I_t < I_{b_max}) \text{ then } I_{co} = 0 \\ \text{If } (I_t > 0) \text{ and } (I_t > I_{b_max}) \text{ and } (SOC_{sc} > SOC_{sc_min}) \text{ then } I_{co} = (I_t - I_{b_max}) \\ \text{If } (I_t < 0) \text{ and } (SOC_{sc} < SOC_{sc_max}) \text{ then } I_{co} = I_t \end{cases} \quad (1)$$

where

$I_t \approx$ total load current of the vehicle.

$I_{co} \approx$ output current of DC-DC converter.

$I_{b_max} \approx$ maximum battery current.

$V_{co} \approx$ output voltage of DC-DC converter.

$SOC_B \approx$ battery state of charge.

$SOC_{sc} \approx$ supercapacitor state of charge.

The standard rule-based algorithm enables the HESS to deliver current from the battery to the EV when the total load current of the EV is below the maximum battery current value (I_{b_max}). It also restricts the battery current to I_{b_max} during high-load drive cycles. Furthermore, the algorithm utilizes the supercapacitor to capture all regenerative energy during deceleration in the drive cycle. The amount of regenerative energy absorbed by the supercapacitor, ranging from its initial voltage to its final voltage, is computed according to Equation (2). Additionally, the algorithm establishes the state of charge condition for the supercapacitor, as specified in Equation (3). Figure 5 illustrates the flowchart for the standard rule-based algorithm.

$$\Delta E_{nSC} = \frac{C_0}{2} (V_{sc}(0)^2 - V_{sc}(t)^2) \quad (2)$$

$$SC_{soc_max} \geq SC_{soc} > SC_{soc_min} \quad (3)$$

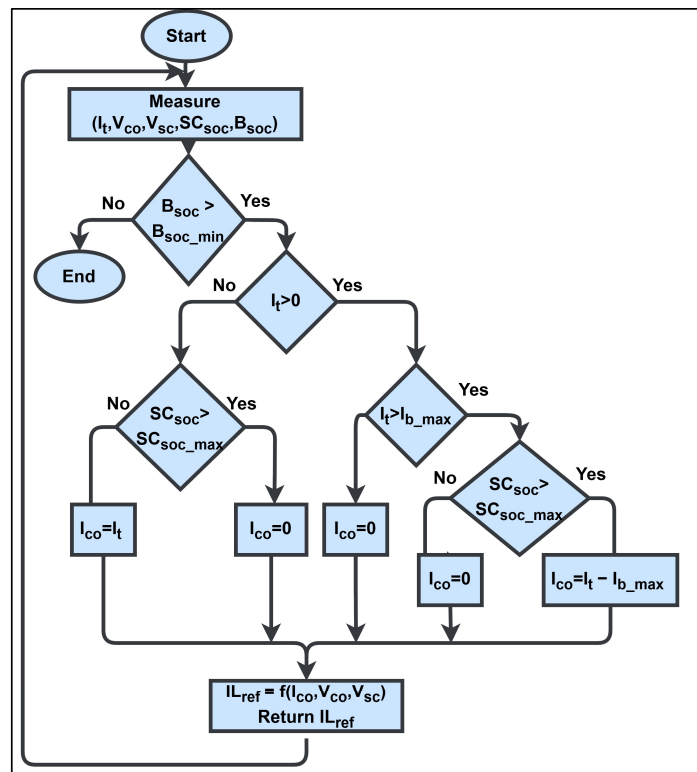


Figure 5. The standard rule-based algorithm flowchart.

3.2. The Adaptive Rule-Based Algorithm of the HESS

An adaptive control method is employed to enhance system performance by dynamically adjusting the algorithm’s coefficients. This adaptive algorithm determines the total current demand required for a specific drive cycle, as well as the regenerative current, by taking into account factors such as the electric vehicle (EV) model parameters, vehicle speed, and road slope. In the HESS, the allocation of energy between the battery and the supercapacitor is independently optimized. The energy management system (EMS) estimates the potential regenerative energy and establishes an energy-sharing ratio (R) between the battery and the supercapacitor, ensuring the HESS operates efficiently and that the supercapacitor captures all regenerative energy during the chosen drive cycle. The energy-sharing ratio (R) in the adaptive rule-based algorithm is adjusted based on the drive cycle. Figure 6 presents the flowchart of the adaptive rule-based algorithm. The supercapacitor supports the battery by supplying the electric vehicle (EV) load current, with the energy-sharing percentage (R) varying across different drive cycles. The EMS continuously monitors the actual EV load current and the supercapacitor’s state of charge to determine the appropriate energy-sharing ratio within the HESS.

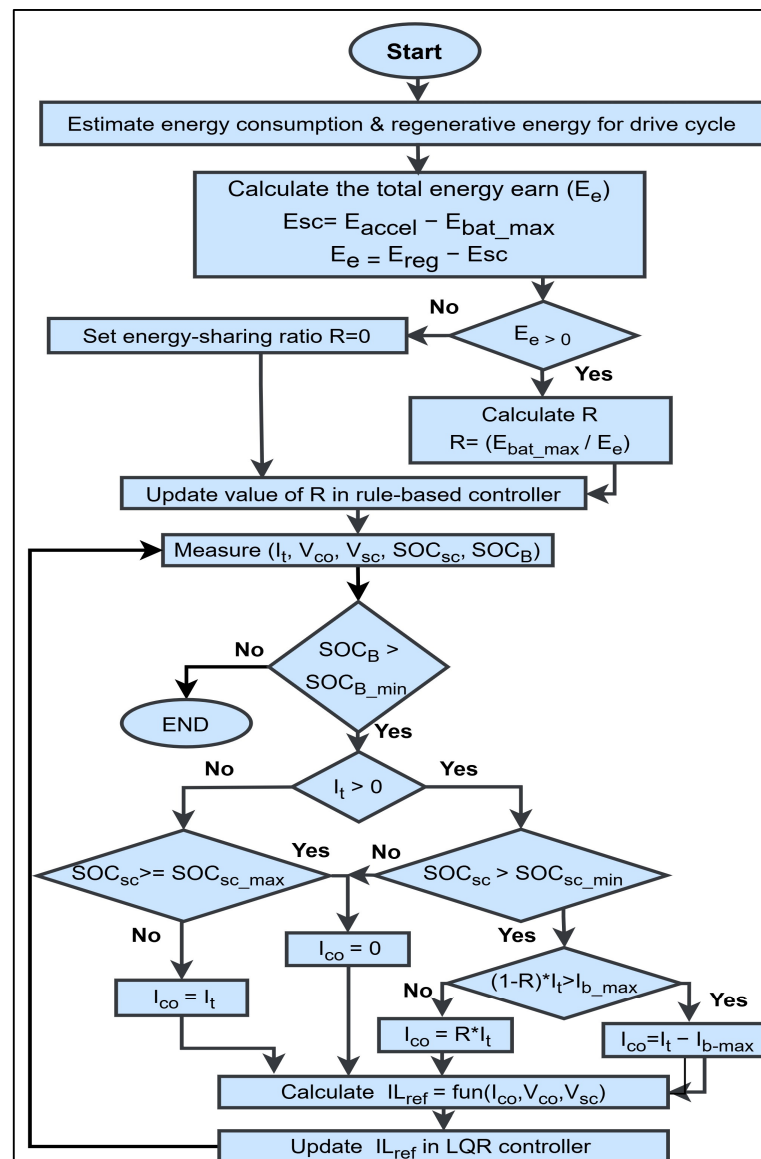


Figure 6. An adaptive rule-based algorithm flowchart.

3.3. The Advanced Adaptive Rule-Based Algorithm of the HESS

The proposed adaptive rule-based algorithm determines the energy-sharing ratio (R) between the battery and supercapacitor by estimating the regenerative energy from the selected drive cycle. In the enhanced version of this algorithm, both the energy-sharing ratio (R) and the maximum allowable battery current (I_{b_max}) are adjusted based on the amount of regenerative energy available in the drive cycle. This approach ensures that the supercapacitor handles peak loads and works alongside the battery to manage the transient load demands of the electric vehicle (EV). The primary goal of this control algorithm is to maximize the reuse of regenerative energy within the same drive cycle, ensuring sufficient capacity to absorb energy during acceleration. Figure 7 illustrates the flowchart of the proposed advanced adaptive rule-based algorithm.

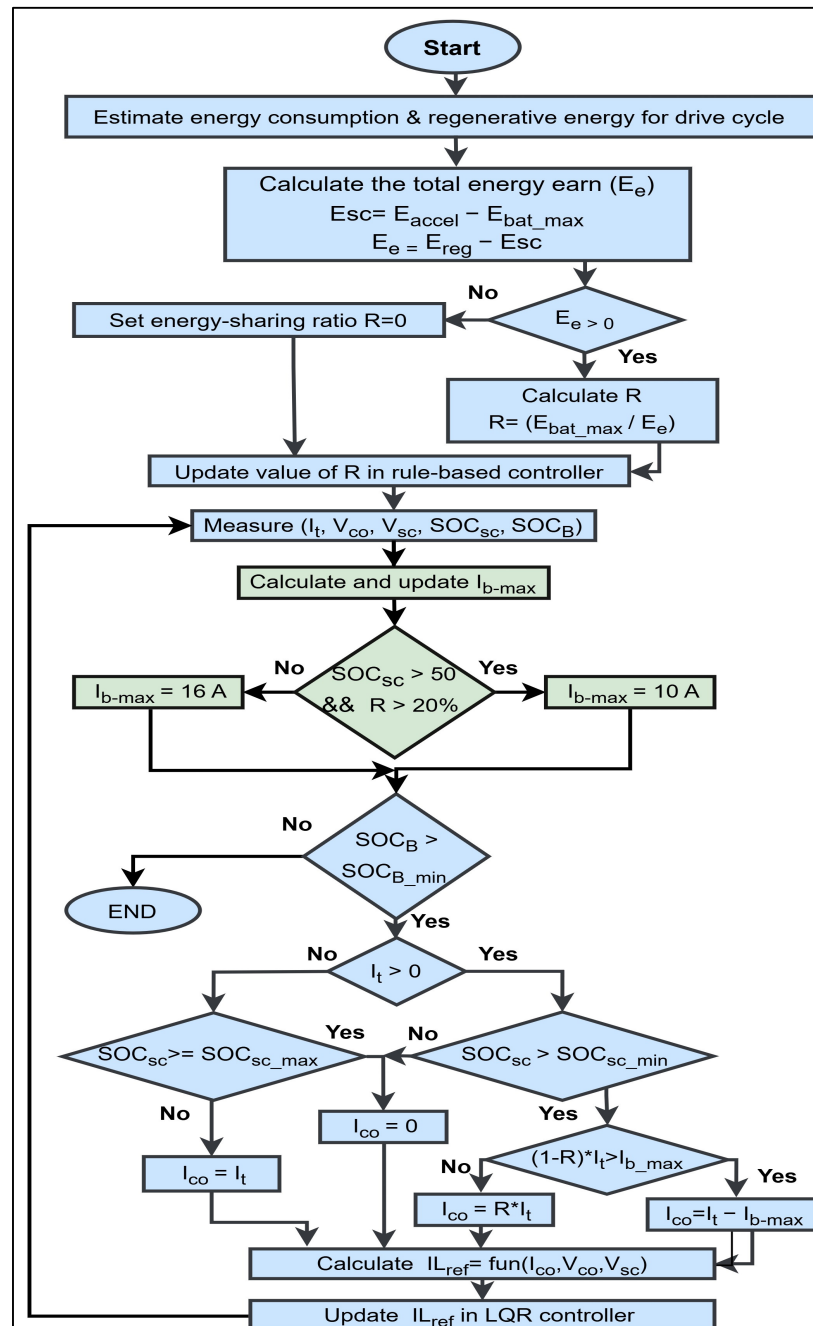
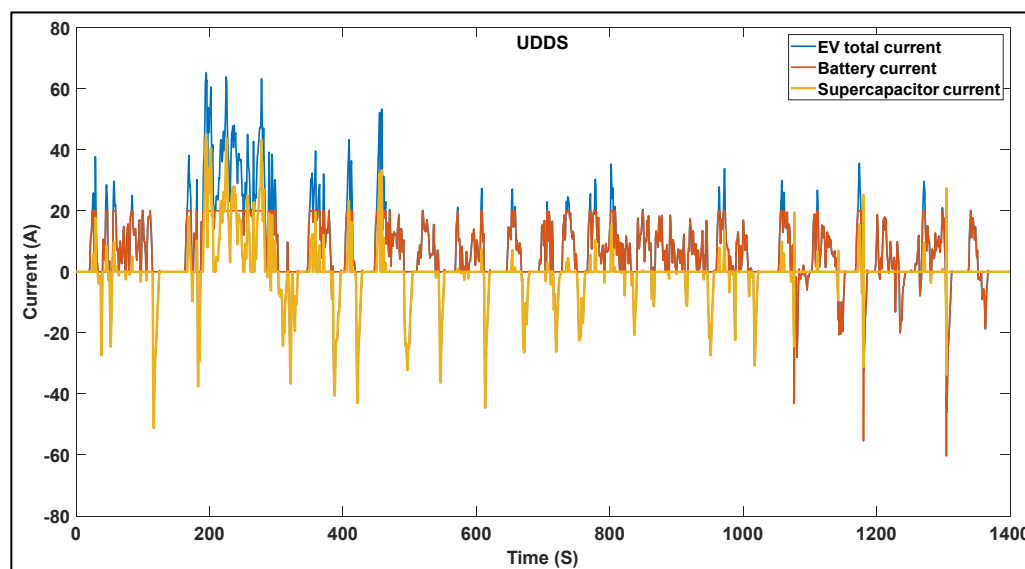


Figure 7. The advanced adaptive rule-based algorithm flowchart.

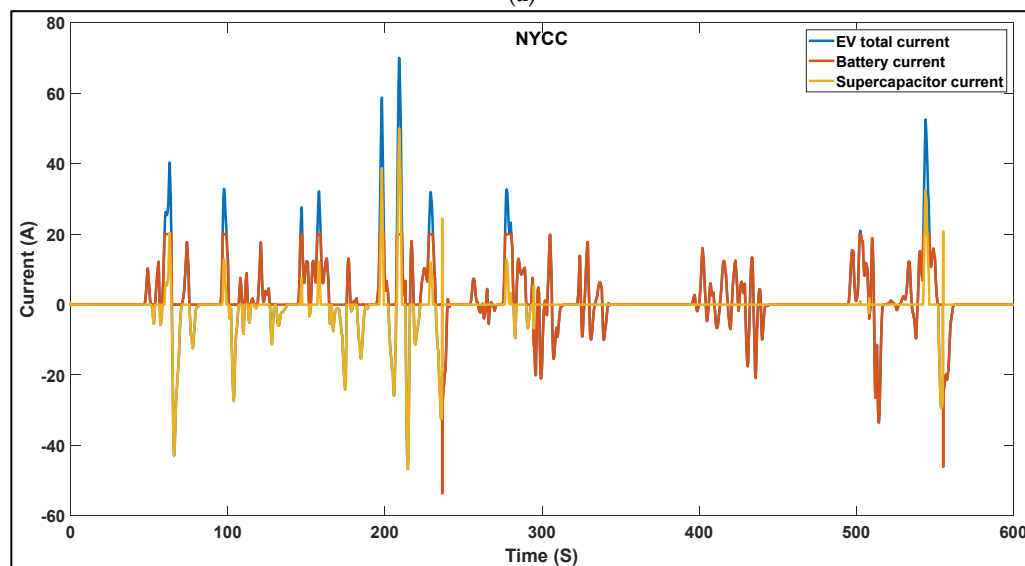
4. Results and Discussion

4.1. The Results of the Standard Rule-Based Algorithm

This section analyzes the performance of the standard rule-based algorithm for the hybrid energy storage system across three different standard drive cycles: UDDS, NYCC, and Japan1015. The total current demand in the electric vehicle (EV) varies in response to the vehicle’s speed profile. In this setup, the battery supplies the low load current, while the supercapacitor manages the peak load demands. Additionally, during deceleration, the supercapacitor captures regenerative energy. Figure 8 illustrates the EV’s overall load current, along with the corresponding currents from the battery and supercapacitor, across the UDDS, NYCC, and Japan1015 drive cycles.



(a)



(b)

Figure 8. Cont.

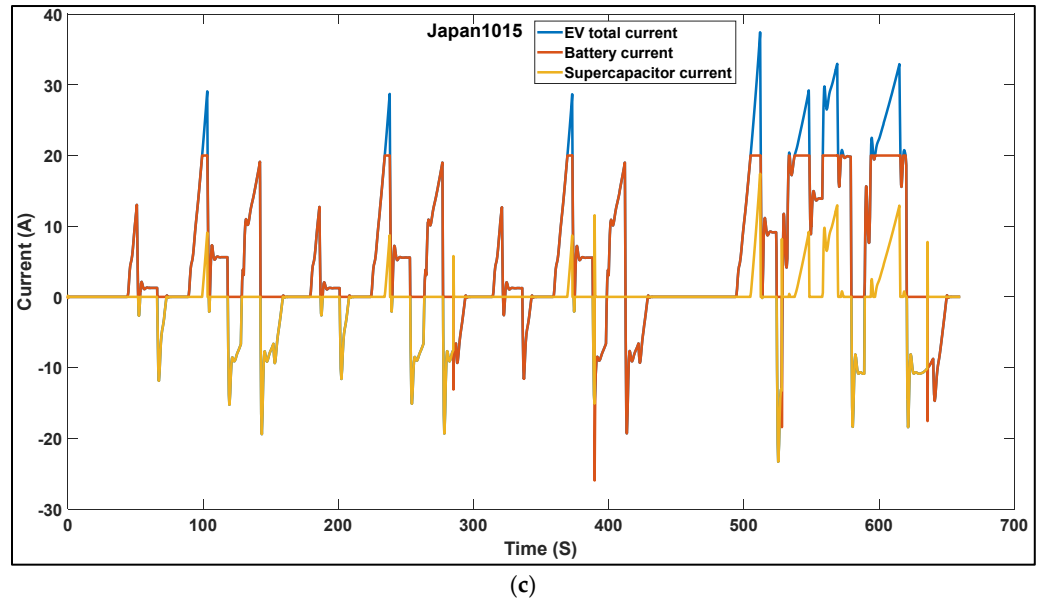


Figure 8. HESS currents during first case using the standard rule-based algorithm for (a) UDDS, (b) NYCC, and (c) Japan1015.

Figure 9 shows the variations in the battery state of charge in the UDDS, NYCC, and Japan1015 drive cycles. After completing one cycle in the first case, the final battery SOC is 0.9258 for UDDS, 0.947 for NYCC, and 0.942 for Japan1015.

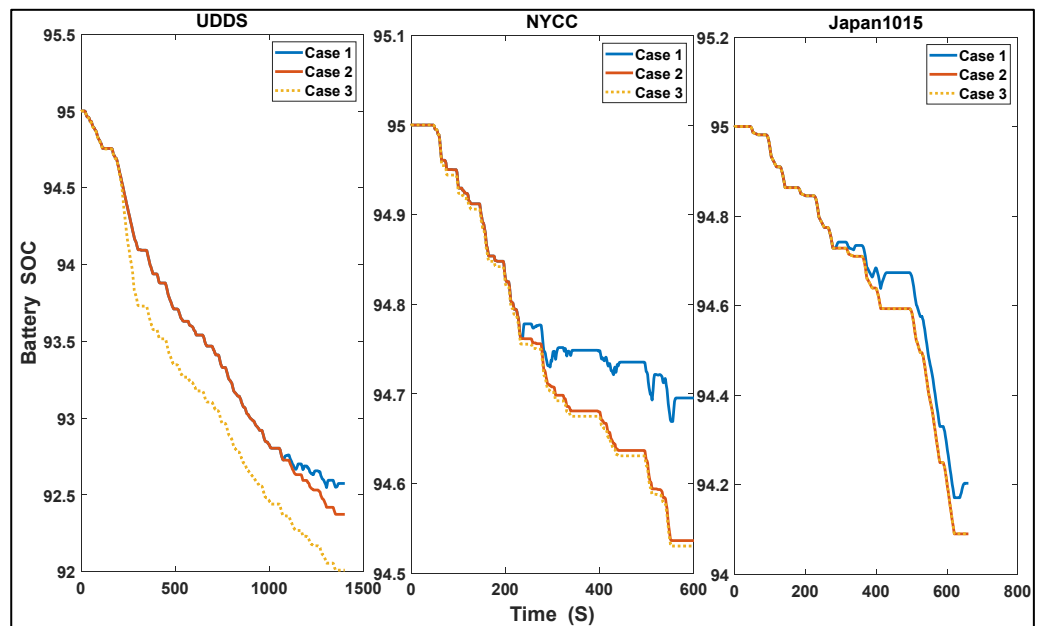


Figure 9. The battery states of charge in the three cases using the standard rule-based algorithm for UDDS, NYCC, and Japan1015 drive cycles.

Figure 10 illustrates the changes in the supercapacitor’s state of charge across the three cases during the UDDS, NYCC, and Japan1015 drive cycles. The supercapacitor discharges to supply high-load currents and recharges by capturing regenerative energy. In the first case, the final state of charge reaches a peak of 0.95 for all drive cycles, showing that the HESS with the rule-based algorithm efficiently recovers energy. Additionally, in the second and third cases, the supercapacitor gains energy during the UDDS, NYCC, and Japan1015 drive cycles.

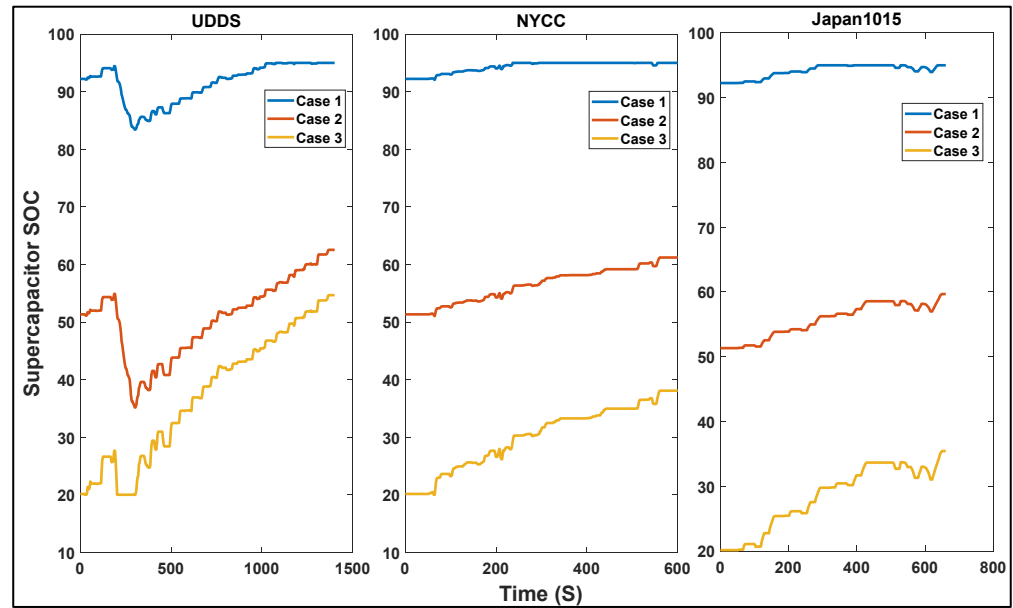


Figure 10. The supercapacitor states of charge in the three cases using the standard rule-based algorithm for UDDS, NYCC, and Japan1015 drive cycles.

Table 4 provides a summary of the energy consumption for the HESS, battery, and supercapacitor under the standard rule-based algorithm during the UDDS, NYCC, and Japan1015 drive cycles. In the first scenario, battery consumption rates were 2.55%, 0.32%, and 0.84% for the UDDS, NYCC, and Japan1015 cycles, respectively. In the second and third scenarios, battery consumption percentages increased across all three drive cycles: UDDS, NYCC, and Japan1015.

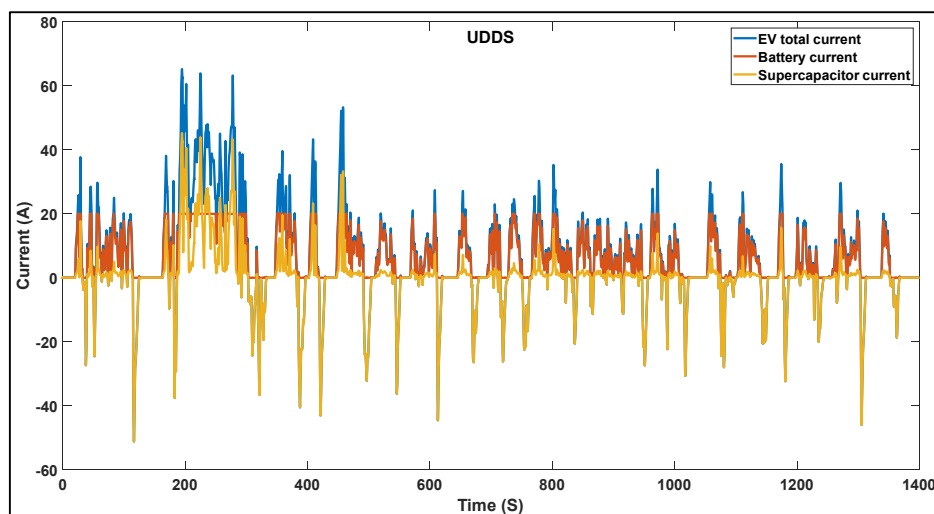
Table 4. HESS results using the standard rule-based algorithm for UDDS, NYCC, and Japan1015 drive cycles.

<i>Initial SCsoc(0)</i>		<i>UDDS</i>	<i>NYCC</i>	<i>Japan1015</i>
<i>1st Case</i> <i>SCsoc = 92%</i>	$SOC_b(t) \%$	92.58	94.7	94.2
	$SOC_{sc}(t) \%$	95	95	95
	<i>Battery Consumption %</i>	2.55	0.32	0.84
	<i>Supercapacitor Consumption %</i>	−3	−3	−3
<i>2nd Case</i> <i>SCsoc = 51%</i>	$SOC_b(t) \%$	92.37	94.54	94.09
	$SOC_{sc}(t) \%$	62.55	61.22	59.68
	<i>Battery Consumption %</i>	2.77	0.48	0.96
	<i>Supercapacitor Consumption %</i>	−21.83	−19.24	−16.24
<i>3rd Case</i> <i>SCsoc = 20%</i>	$SOC_b(t) \%$	92.01	94.53	94.09
	$SOC_{sc}(t) \%$	54.69	38.08	35.43
	<i>Battery Consumption %</i>	3.15	0.5	0.96
	<i>Supercapacitor Consumption %</i>	−171	−89	−76

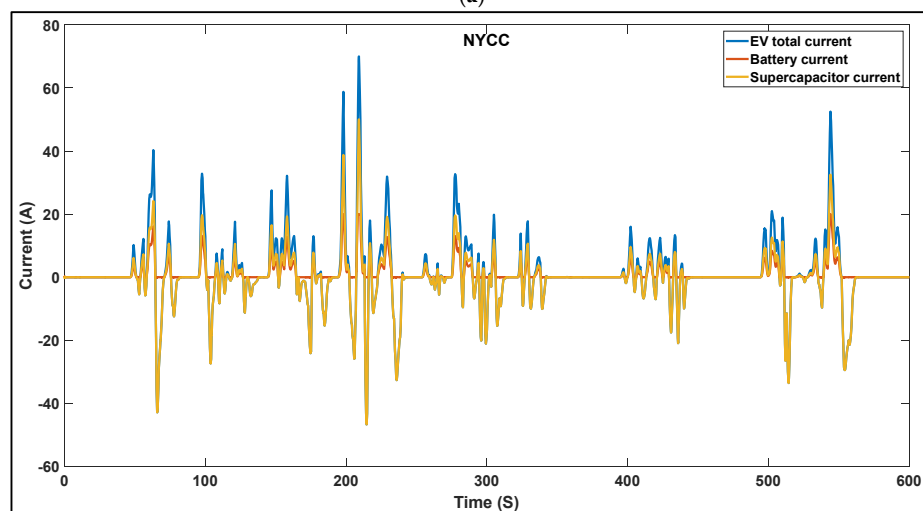
4.2. The Results of the Adaptive Rule-Based Algorithm

This section examines the HESS performance using the adaptive rule-based algorithm across three different drive cycles. During these cycles, the energy sharing between the battery and supercapacitor under low load conditions is continuously estimated and adjusted according to the vehicle’s speed. Figure 11 displays the EV’s total load current, as well as the battery and supercapacitor currents for the first case throughout the UDDS, NYCC, and Japan1015 cycles. The results demonstrate that the adaptive rule-based algorithm

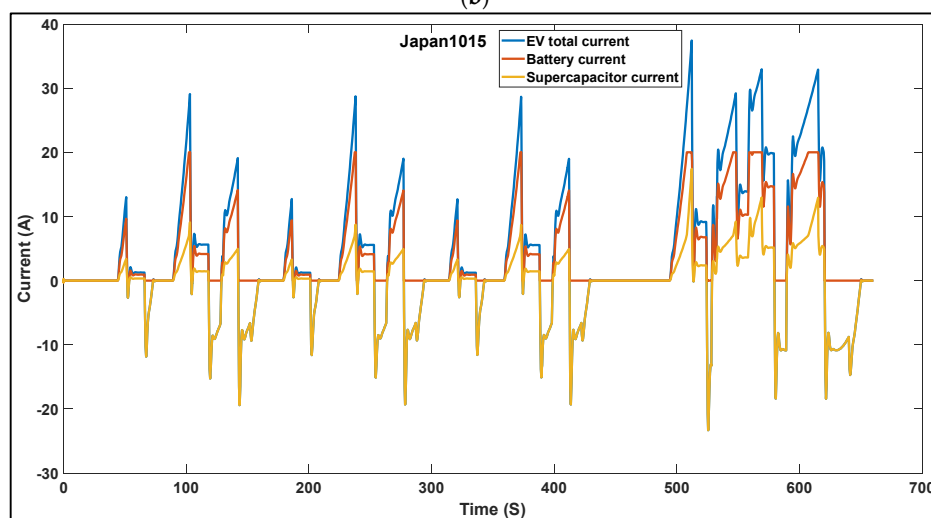
effectively minimized battery strain compared to a system using only a battery, keeping the battery current within the maximum limit (I_{b_max}) during the drive.



(a)



(b)



(c)

Figure 11. HESS currents during first case using the adaptive rule-based algorithm for (a) UDDS, (b) NYCC, and (c) Japan1015.

Figure 12 shows the variations in battery state of charge (SoC) across three scenarios during the UDDS, NYCC, and Japan1015 drive cycles using the adaptive rule-based algorithm. At the end of a single drive cycle in the first scenario, the final battery SoC is 0.9285 for UDDS, 0.9478 for NYCC, and 0.9426 for Japan1015. In comparison, the standard rule-based algorithm resulted in higher battery energy consumption than the adaptive algorithm. Furthermore, battery consumption remained the same in the first and second scenarios for all three drive cycles but increased in the third scenario.

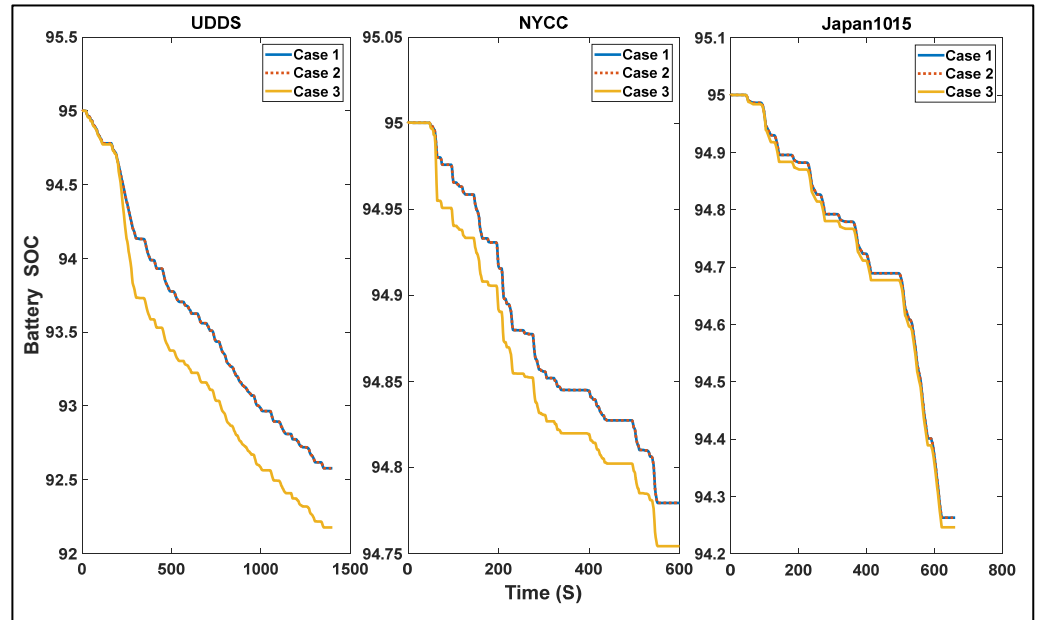


Figure 12. The battery states of charge in the three cases using the adaptive rule-based algorithm for UDDS, NYCC, and Japan1015 drive cycles.

In the first scenario, the final supercapacitor SoC for the UDDS, NYCC, and Japan1015 cycles is 0.95, 0.9308, and 0.9365, respectively. These findings indicate that the supercapacitor within the HESS system, managed by the adaptive rule-based algorithm, effectively captures and stores energy across all tested drive cycles. Figure 13 illustrates the changes in the supercapacitor SoC across the three scenarios for the UDDS, NYCC, and Japan1015 cycles. The results highlight the supercapacitor’s efficiency in balancing energy demands and maximizing regenerative energy recovery under varying load conditions.

Table 5 summarizes the total energy consumption of the battery and supercapacitor across three different initial states of charge (SOCs) for the supercapacitor: high, moderate, and low, using the adaptive rule-based algorithm during the UDDS, NYCC, and Japan1015 drive cycles. This adaptive algorithm is designed to optimize the use of regenerative energy stored in the supercapacitor to assist the battery in meeting the load demands of the electric vehicle (EV). The results from all three cases demonstrate that the adaptive rule-based algorithm effectively manages the supercapacitor’s energy across various SOC levels.

Table 5. HESS results using the adaptive rule-based algorithm for UDDS, NYCC, and Japan1015 drive cycles.

Initial SCsoc(0)		UDDS	NYCC	Japan1015
1st Case	SOC _b (t) %	92.58	94.78	94.26
	SOC _{sc} (t) %	95	93.08	93.65
SCsoc = 92%	Battery Consumption %	2.55%	0.23%	0.78%
	Supercapacitor Consumption %	−3	−0.91%	−1.53%

Table 5. Cont.

Initial SCsoc(0)		UDDS	NYCC	Japan1015
2nd Case SCsoc = 51%	SOC _b (t) %	92.58	94.78	94.26
	SOC _{sc} (t) %	55.68	52.7	53.62
	Battery Consumption %	2.55%	0.23%	0.78%
	Supercapacitor Consumption %	−8.45%	−2.63%	−4.44%
3rd Case SCsoc = 20%	SOC _b (t) %	92.18	94.75	94.25
	SOC _{sc} (t) %	48.39	24.88	26.11
	Battery Consumption %	2.97%	0.26%	0.79%
	Supercapacitor Consumption %	−140%	−23.5%	−29.6%

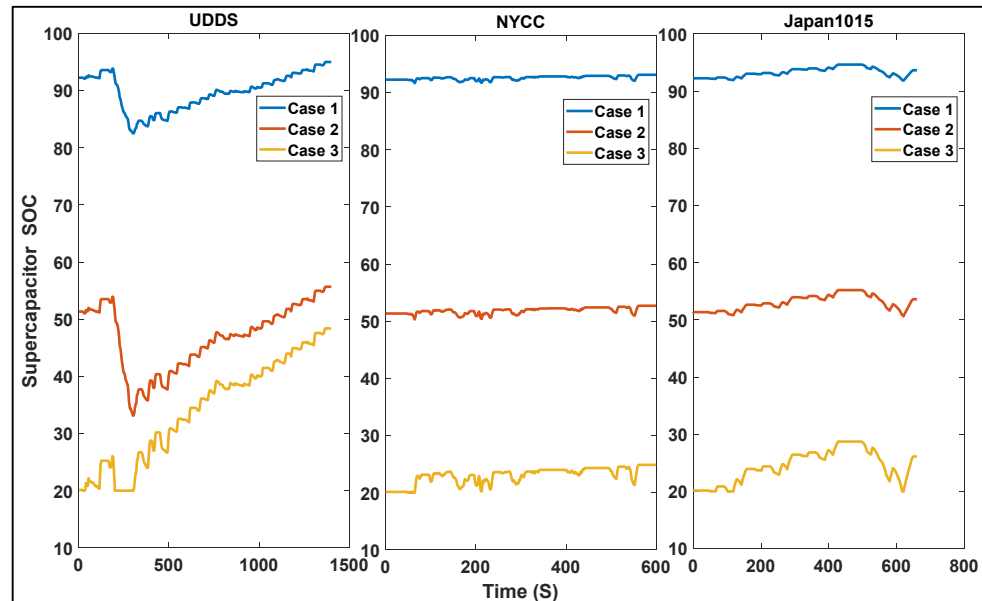
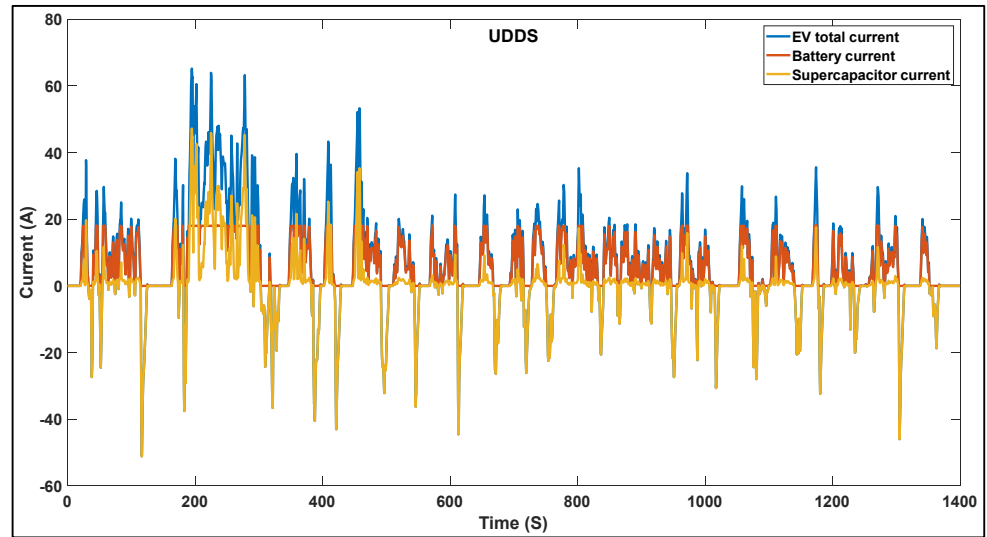


Figure 13. The supercapacitor states of charge in the three cases using the adaptive rule-based algorithm for UDDS, NYCC, and Japan1015 drive cycles.

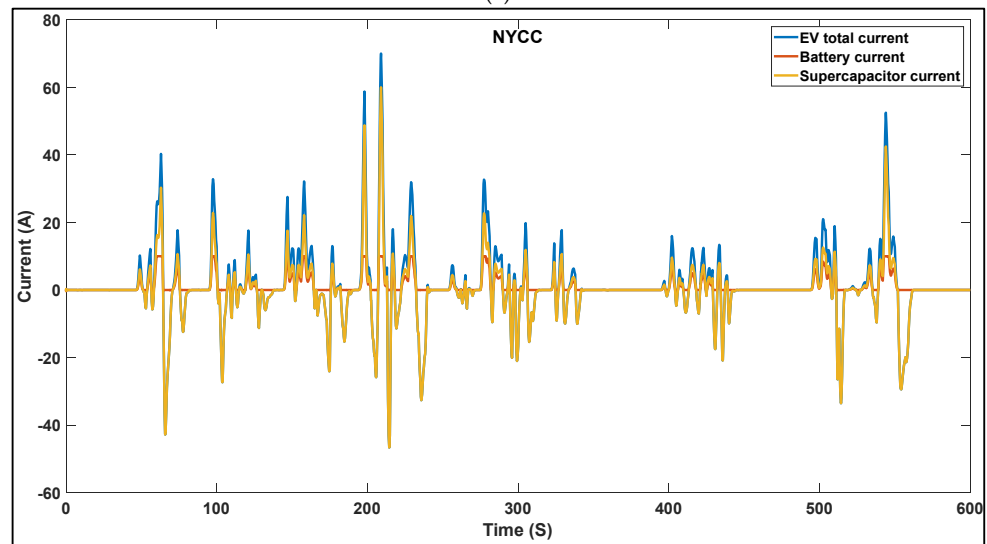
4.3. The Results of the Advanced Adaptive Rule-Based Algorithm

This section evaluates the performance of the HESS using the advanced adaptive rule-based algorithm across three standard drive cycles. In these cycles, both the battery and supercapacitor handle the low load current, while the supercapacitor manages peak load demands and captures regenerative energy during deceleration. The advanced adaptive rule-based algorithm was specifically designed to extend the number of drive cycles. The key difference between the advanced adaptive and the standard adaptive algorithms lies in their flexibility. While the standard adaptive algorithm adjusts only the energy-sharing percentage between the battery and supercapacitor, the advanced adaptive algorithm dynamically modifies both the maximum battery current and the energy-sharing ratio in response to the drive cycle. For the UDDS, NYCC, and Japan1015 cycles, the energy-sharing percentages between the battery and supercapacitor are 0.12, 0.6, and 0.26, respectively. Figure 14 presents the total EV load current, along with the battery and supercapacitor currents, for the first scenario during the UDDS, NYCC, and Japan1015 drive cycles.

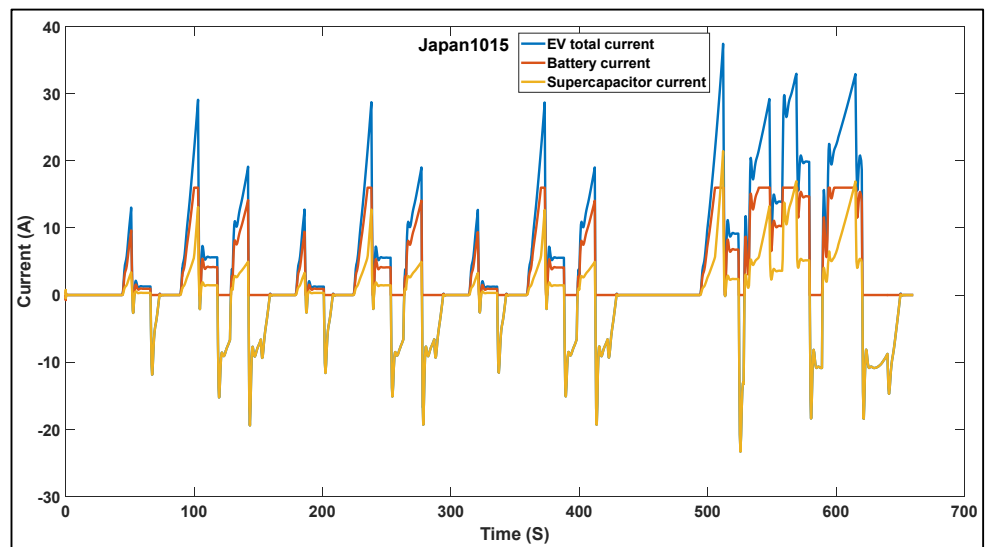
Figure 15 illustrates the changes in battery state of charge (SoC) across three scenarios during the UDDS, NYCC, and Japan1015 drive cycles. In the first scenario, the final battery SoC after a single drive cycle is 0.9267 for UDDS, 0.9480 for NYCC, and 0.9431 for Japan1015. Compared to the standard rule-based and adaptive rule-based algorithms, the advanced adaptive rule-based algorithm resulted in lower battery energy consumption across different supercapacitor SoC levels during the three standard drive cycles.



(a)



(b)



(c)

Figure 14. HESS currents during first case using the advanced adaptive rule-based algorithm for (a) UDDS, (b) NYCC, and (c) Japan1015.

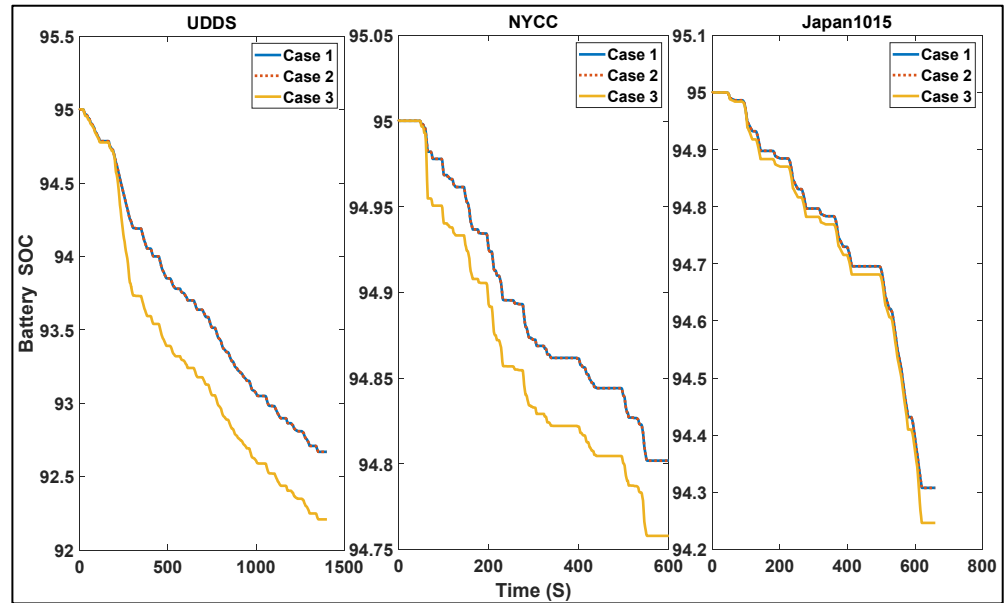


Figure 15. The battery states of charge in the three cases using the advanced adaptive rule-based algorithm for UDDS, NYCC, and Japan1015 drive cycles.

On the other hand, the final SoC of the supercapacitor in the first scenario is 0.9286 for UDDS, 0.9256 for NYCC, and 0.9263 for Japan1015. These results indicate that the supercapacitor within the HESS, managed by the advanced adaptive rule-based algorithm, effectively captures and stores energy throughout all tested drive cycles. Figure 16 shows the variations in the supercapacitor’s SoC across the three scenarios during the UDDS, NYCC, and Japan1015 drive cycles.

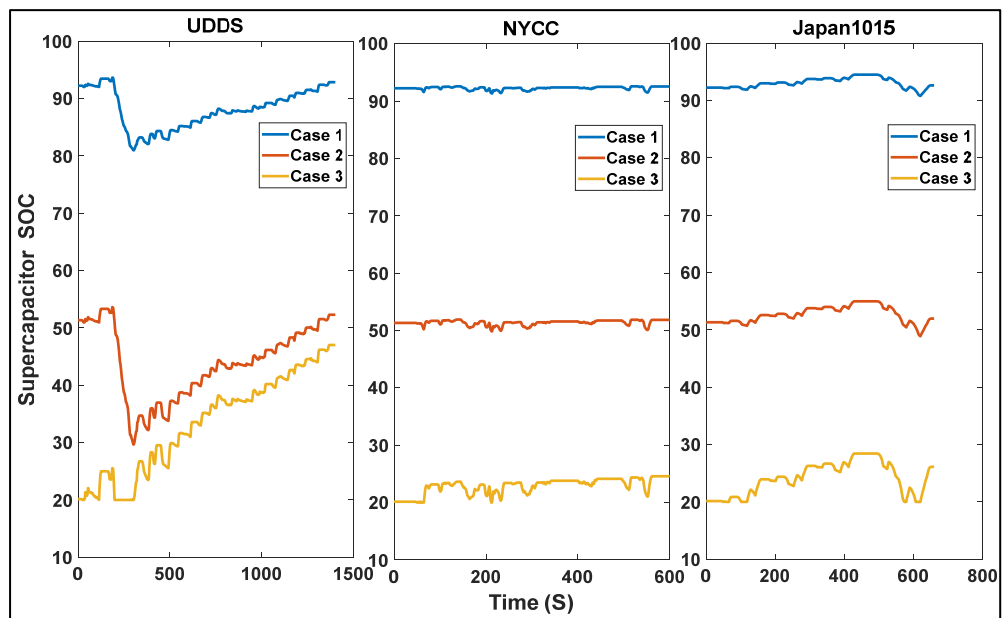


Figure 16. The supercapacitor states of charge in the three cases using the advanced adaptive rule-based algorithm for UDDS, NYCC, and Japan1015 drive cycles.

Table 6 presents the total energy consumption of the battery and supercapacitor in the HESS, which employs the advanced adaptive rule-based algorithm, across three different initial states of charge (SOCs) for the supercapacitor during the UDDS, NYCC, and Japan1015 drive cycles. In the first scenario, the battery energy consumption is recorded

at 2.45% for UDDS, 0.21% for NYCC, and 0.75% for Japan1015. These findings demonstrate that the advanced adaptive rule-based algorithm significantly reduces battery energy consumption compared to both the standard and adaptive rule-based algorithms across all drive cycles. The proposed advanced algorithm effectively manages energy sharing between the battery and supercapacitor in the HESS for an electric vehicle (EV), accommodating various initial SOC levels of the supercapacitor.

Table 6. HESS results using the advanced adaptive rule-based algorithm for UDDS, NYCC, and Japan1015 drive cycles.

Initial SCsoc(0)		UDDS	NYCC	Japan1015
1st Case SCsoc = 92%	SOC _b (t) %	92.67	94.8	94.31
	SOC _{sc} (t) %	92.86	92.56	92.63
	Battery Consumption %	2.45%	0.21%	0.75%
	Supercapacitor Consumption %	−0.67%	−0.35%	−0.42%
2nd Case SCsoc = 51%	SOC _b (t) %	92.67	94.8	94.31
	SOC _{sc} (t) %	52.28	51.85	51.96
	Battery Consumption %	2.45%	0.21%	0.75%
	Supercapacitor Consumption %	−1.77%	−1%	−1.2%
3rd Case SCsoc = 20%	SOC _b (t) %	92.21	94.76	94.25
	SOC _{sc} (t) %	47.02	24.6	26.11
	Battery Consumption %	2.93%	0.25%	0.79%
	Supercapacitor Consumption %	−133%	−22.08	−29.6%

Finally, the performance of the proposed algorithm was evaluated through three standard drive cycles: UDDS, NYCC, and Japan1015. Figure 17 illustrates the comparison of the battery states of charge using the standard rule-based algorithm, the adaptive rule-based algorithm, and the advanced adaptive rule-based algorithm.

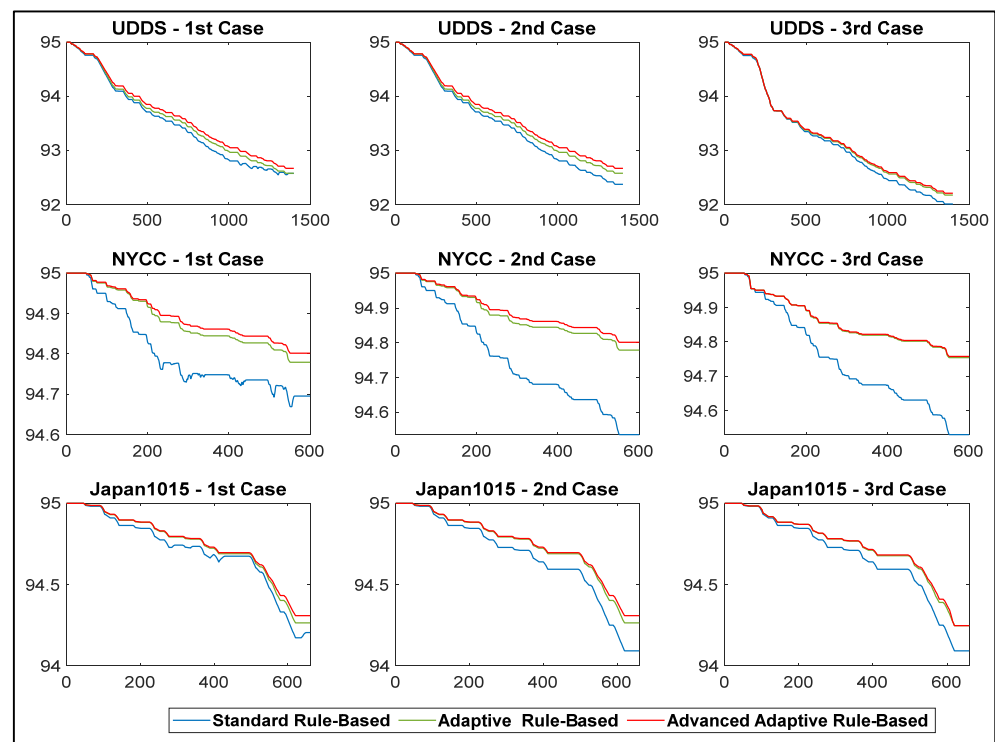


Figure 17. Comparison of the battery states of charge in the three cases using the three rule-based algorithms for UDDS, NYCC, and Japan1015 drive cycles.

Table 7 presents a summary of the potential cycles achieved across three distinct cases utilizing the standard rule-based algorithm, the adaptive rule-based algorithm, and the advanced adaptive rule-based algorithm.

Table 7. The estimated number of available cycles using the presented algorithms.

Drive Cycle	Initial SCsoc(0)	Standard Rule-Based	Adaptive Rule-Based	Advanced Adaptive Rule-Based
UDDS	1st Case	29	29	30
	2nd Case	27	29	30
	3rd Case	24	25	26
NYCC	1st Case	234	326	357
	2nd Case	156	326	357
	3rd Case	150	288	300
Japan1015	1st Case	89	96	100
	2nd Case	78	96	100
	3rd Case	78	95	95

In the first case, the standard adaptive rule-based algorithm enabled the HESS of EV to complete 29 drive cycles for UDDS, 234 for NYCC, and 89 for Japan1015. In contrast, the advanced rule-based algorithm significantly enhanced these results, allowing for 30 drive cycles for UDDS, 357 for NYCC, and 100 for Japan1015. Moreover, this advanced algorithm also proved effective in extending the number of drive cycles in the second and third cases for all three cycles: UDDS, NYCC, and Japan1015. This demonstrates the advanced adaptive rule-based algorithm's superior capability in optimizing energy management and performance in varied driving conditions.

5. Conclusions

This research presents a novel energy management strategy for hybrid energy storage systems in electric vehicles, utilizing a multi-layer control approach. This study introduces three distinct types of rule-based algorithms: a standard rule-based algorithm, an adaptive rule-based algorithm, and an advanced adaptive rule-based algorithm. The standard rule-based algorithm operates with fixed parameters that do not account for the topographical characteristics of the route. In contrast, the adaptive rule-based algorithm adjusts its parameters based on the amount of regenerative energy that can be absorbed during the journey. The advanced adaptive rule-based algorithm continuously updates its parameters according to the specific drive cycle selected. To evaluate the performance of these control strategies, simulations were conducted with various initial states of charge for the supercapacitor, set at 92% for high SCSOC, 51% for moderate SCSOC, and 20% for low SCSOC. The tests were carried out using three standard drive cycles: UDDS, NYCC, and Japan1015. The results reveal that the standard rule-based algorithm effectively mitigates current peaks and reduces battery energy consumption when compared to a system relying solely on a single energy storage battery. The adaptive rule-based algorithm also demonstrates improvements in reducing battery current peaks and overall consumption. However, the advanced adaptive algorithm stands out by not only decreasing the battery current peaks but also increasing the number of possible drive cycles compared with the performance of the other two algorithms. For future research, the proposed control algorithms will be implemented in an electric vehicle prototype to further validate the simulation results, ensuring their practical applicability and effectiveness in real-world situations.

Author Contributions: Conceptualization, T.S. and C.K.W.; methodology, T.S.; software, T.S.; validation, T.S. and C.K.W.; formal analysis, T.S.; investigation, T.S.; resources, T.S. and C.K.W.; data curation,

T.S.; writing—original draft preparation, C.K.W.; writing—review and editing, T.S.; visualization, T.S. and C.K.W.; supervision, C.K.W. and L.C.H.; project administration, C.K.W.; funding acquisition, C.K.W. and L.C.H. All authors have read and agreed to the published version of the manuscript.

Funding: This research was funded by UTARRF, grant number 8012/001, Universiti Tunku Abdul Rahman (UTAR).

Data Availability Statement: Data will be made available on request.

Conflicts of Interest: The authors declare no conflicts of interest.

References

1. Tran, M.-K.; Bhatti, A.; Vrolyk, R.; Wong, D.; Panchal, S.; Fowler, M.; Fraser, R. A review of range extenders in battery electric vehicles: Current progress and future perspectives. *World Electr. Veh. J.* **2021**, *12*, 54. [[CrossRef](#)]
2. Javadi, M.; Liang, X.; Gong, Y.; Chung, C.Y. Battery energy storage technology in renewable energy integration: A review. In Proceedings of the 2022 IEEE Canadian Conference on Electrical and Computer Engineering (CCECE), Halifax, NS, Canada, 18–20 September 2022; IEEE: Piscataway, NJ, USA, 2022; pp. 435–440.
3. Devillers, N.; Jemei, S.; Péra, M.-C.; Bienaimé, D.; Gustin, F. Review of characterization methods for supercapacitor modelling. *J. Power Sources* **2014**, *246*, 596–608. [[CrossRef](#)]
4. Fotouhi, A.; Propp, K.; Auger, D.J. Electric vehicle battery model identification and state of charge estimation in real world driving cycles. In Proceedings of the 2015 7th Computer Science and Electronic Engineering Conference (CEEC), Colchester, UK, 24–25 September 2015; IEEE: Piscataway, NJ, USA, 2015; pp. 243–248.
5. Ren, G.; Shan, S.; Ma, G.; Shang, X.; Zhu, S.; Zhang, Q.; Yang, T. Review of energy storage technologies for extended range electric vehicle. *J. Appl. Sci. Eng.* **2019**, *22*, 69–82.
6. Udhaya Sankar, G.; Moorthy, C.G.; RajKumar, G. Smart storage systems for electric vehicles—A review. *Smart Sci.* **2019**, *7*, 1–15. [[CrossRef](#)]
7. Balog, R.S.; Davoudi, A. Batteries, battery management, and battery charging technology. In *Electric, Hybrid, and Fuel Cell Vehicles*; Springer: Berlin/Heidelberg, Germany, 2021; pp. 315–352.
8. Pearre, N.S.; Kempton, W.; Guensler, R.L.; Elango, V.V. Electric vehicles: How much range is required for a day's driving? *Transp. Res. Part C Emerg. Technol.* **2011**, *19*, 1171–1184. [[CrossRef](#)]
9. Neubauer, J.; Pesaran, A.; Bae, C.; Elder, R.; Cunningham, B. Updating United States Advanced Battery Consortium and Department of Energy battery technology targets for battery electric vehicles. *J. Power Sources* **2014**, *271*, 614–621. [[CrossRef](#)]
10. Schaltz, E.; Soylu, S. Electrical vehicle design and modeling. In *Electric Vehicles-Modelling and Simulations*; IntechOpen: London, UK, 2011; Volume 1, pp. 1–24.
11. Jordán, J.; Palanca, J.; Del Val, E.; Julian, V.; Botti, V. A multi-agent system for the dynamic emplacement of electric vehicle charging stations. *Appl. Sci.* **2018**, *8*, 313. [[CrossRef](#)]
12. Veneri, O.; Capasso, C.; Patalano, S. Experimental investigation into the effectiveness of a super-capacitor based hybrid energy storage system for urban commercial vehicles. *Appl. Energy* **2018**, *227*, 312–323. [[CrossRef](#)]
13. Li, Y.; Huang, X.; Liu, D.; Wang, M.; Xu, J. Hybrid energy storage system and energy distribution strategy for four-wheel independent-drive electric vehicles. *J. Clean. Prod.* **2019**, *220*, 756–770. [[CrossRef](#)]
14. Capasso, C.; Lauria, D.; Veneri, O. Experimental evaluation of model-based control strategies of sodium-nickel chloride battery plus supercapacitor hybrid storage systems for urban electric vehicles. *Appl. Energy* **2018**, *228*, 2478–2489. [[CrossRef](#)]
15. Wang, C.; Liu, R.; Tang, A. Energy management strategy of hybrid energy storage system for electric vehicles based on genetic algorithm optimization and temperature effect. *J. Energy Storage* **2022**, *51*, 104314. [[CrossRef](#)]
16. Rezaei, H.; Abdollahi, S.E.; Abdollahi, S.; Filizadeh, S. Energy management strategies of battery-ultracapacitor hybrid storage systems for electric vehicles: Review, challenges, and future trends. *J. Energy Storage* **2022**, *53*, 105045. [[CrossRef](#)]
17. Xiang, C.; Wang, Y.; Hu, S.; Wang, W. A new topology and control strategy for a hybrid battery-ultracapacitor energy storage system. *Energies* **2014**, *7*, 2874–2896. [[CrossRef](#)]
18. Tie, S.F.; Tan, C.W. A review of energy sources and energy management system in electric vehicles. *Renew. Sustain. Energy Rev.* **2013**, *20*, 82–102. [[CrossRef](#)]
19. Ju, F.; Zhang, Q.; Deng, W.; Li, J. Review of structures and control of battery-supercapacitor hybrid energy storage system for electric vehicles. In *Advances in Battery Manufacturing, Service, and Management Systems*; John Wiley & Sons: Hoboken, NJ, USA, 2016; pp. 303–318.
20. Cao, J.; Emadi, A. A new battery/ultracapacitor hybrid energy storage system for electric, hybrid, and plug-in hybrid electric vehicles. *IEEE Trans. Power Electron.* **2011**, *27*, 122–132.

21. Ostadi, A.; Kazerani, M.; Chen, S.-K. Hybrid Energy Storage System (HESS) in vehicular applications: A review on interfacing battery and ultra-capacitor units. In Proceedings of the 2013 IEEE Transportation Electrification Conference and Expo (ITEC), Metro Detroit, MI, USA, 16–19 June 2013; IEEE: Piscataway, NJ, USA, 2013; pp. 1–7.
22. Aharon, I.; Kuperman, A. Topological overview of powertrains for battery-powered vehicles with range extenders. *IEEE Trans. Power Electron.* **2011**, *26*, 868–876. [[CrossRef](#)]
23. Pipicelli, M.; Sessa, B.; De Nola, F.; Gimelli, A.; Di Blasio, G. Assessment of Battery–Supercapacitor Topologies of an Electric Vehicle under Real Driving Conditions. *Vehicles* **2023**, *5*, 424–445. [[CrossRef](#)]
24. Iannuzzi, D.; Tricoli, P. Speed-based state-of-charge tracking control for metro trains with onboard supercapacitors. *IEEE Trans. Power Electron.* **2011**, *27*, 2129–2140. [[CrossRef](#)]
25. Armenta, J.; Núñez, C.; Visairo, N.; Lázaro, I. An advanced energy management system for controlling the ultracapacitor discharge and improving the electric vehicle range. *J. Power Sources* **2015**, *284*, 452–458. [[CrossRef](#)]
26. Kuperman, A.; Aharon, I. Battery–ultracapacitor hybrids for pulsed current loads: A review. *Renew. Sustain. Energy Rev.* **2011**, *15*, 981–992. [[CrossRef](#)]
27. Laldin, O.; Moshirvaziri, M.; Trescases, O. Predictive algorithm for optimizing power flow in hybrid ultracapacitor/battery storage systems for light electric vehicles. *IEEE Trans. Power Electron.* **2012**, *28*, 3882–3895. [[CrossRef](#)]
28. Sadeq, T.; Wai, C.K. Linear quadratic regulator control scheme on hybrid energy storage system. In Proceedings of the 2020 IEEE International Conference on Automatic Control and Intelligent Systems (I2CACIS), Shah Alam, Malaysia, 20 June 2020; IEEE: Piscataway, NJ, USA, 2020; pp. 219–223.
29. Ehsani, M.; Singh, K.V.; Bansal, H.O.; Mehrjardi, R.T. State of the art and trends in electric and hybrid electric vehicles. *Proc. IEEE* **2021**, *109*, 967–984. [[CrossRef](#)]
30. Upadhyaya, A.; Mahanta, C. An Overview of Battery Based Electric Vehicle Technologies with Emphasis on Energy Sources, Their Configuration Topologies and Management Strategies. *IEEE Trans. Intell. Transp. Syst.* **2023**, *25*, 1087–1111. [[CrossRef](#)]
31. Hu, X.; Zou, C.; Zhang, C.; Li, Y. Technological developments in batteries: A survey of principal roles, types, and management needs. *IEEE Power Energy Mag.* **2017**, *15*, 20–31. [[CrossRef](#)]
32. Tian, Y.; Liu, J.; Yao, Q.; Liu, K. Optimal control strategy for parallel plug-in hybrid electric vehicles based on dynamic programming. *World Electr. Veh. J.* **2021**, *12*, 85. [[CrossRef](#)]
33. Abdelaal, A.S.; Mukhopadhyay, S.; Rehman, H. Battery energy management techniques for an electric vehicle traction system. *IEEE Access* **2022**, *10*, 84015–84037. [[CrossRef](#)]
34. Şen, M.; Özcan, M.; Eker, Y.R. Fuzzy Logic-Based Energy Management System for Regenerative Braking of Electric Vehicles with Hybrid Energy Storage System. *Appl. Sci.* **2024**, *14*, 3077. [[CrossRef](#)]
35. Salari, A.H.; Mirzaeinejad, H.; Mahani, M.F. A new control algorithm of regenerative braking management for energy efficiency and safety enhancement of electric vehicles. *Energy Convers. Manag.* **2023**, *276*, 116564. [[CrossRef](#)]
36. Navarro, G.; Torres, J.; Blanco, M.; Nájera, J.; Santos-Herran, M.; Lafoz, M. Present and future of supercapacitor technology applied to powertrains, renewable generation and grid connection applications. *Energies* **2021**, *14*, 3060. [[CrossRef](#)]
37. Sadeq, T.; Wai, C.K.; Morris, E.; Tarbosh, Q.A.; Aydoğdu, Ö. Optimal control strategy to maximize the performance of hybrid energy storage system for electric vehicle considering topography information. *IEEE Access* **2020**, *8*, 216994–217007. [[CrossRef](#)]
38. Chen, X.; Li, M.; Chen, Z. Meta rule-based energy management strategy for battery/supercapacitor hybrid electric vehicles. *Energy* **2023**, *285*, 129365. [[CrossRef](#)]
39. Farrag, M.; Lai, C.S.; Darwish, M.; Taylor, G. Improving the efficiency of electric vehicles: Advancements in hybrid energy storage systems. *Vehicles* **2024**, *6*, 1089–1113. [[CrossRef](#)]
40. Van Jaarsveld, M.J.; Gouws, R. An active hybrid energy storage system utilising a fuzzy logic rule-based control strategy. *World Electr. Veh. J.* **2020**, *11*, 34. [[CrossRef](#)]
41. Kachhwaha, A.; Rashed, G.I.; Garg, A.R.; Mahela, O.P.; Khan, B.; Shafik, M.B.; Hussien, M.G. Design and performance analysis of hybrid battery and ultracapacitor energy storage system for electrical vehicle active power management. *Sustainability* **2022**, *14*, 776. [[CrossRef](#)]
42. Zheng, C.; Wang, Y.; Liu, Z.; Sun, T.; Kim, N.; Jeong, J.; Cha, S.W. A hybrid energy storage system for an electric vehicle and its effectiveness validation. *Int. J. Precis. Eng. Manuf. Green Technol.* **2021**, *8*, 1739–1754. [[CrossRef](#)]
43. Anh, N.T.; Chen, C.-K.; Liu, X. An Efficient Regenerative Braking System for Electric Vehicles Based on a Fuzzy Control Strategy. *Vehicles* **2024**, *6*, 1496–1512. [[CrossRef](#)]
44. Wipke, K.; Cuddy, M.; Bharathan, D.; Burch, S.; Johnson, V.; Markel, A.; Sprik, S. *ADVISOR 2.0: A Second-Generation Advanced Vehicle Simulator for Systems Analysis*; National Renewable Energy Lab. (NREL): Golden, CO, USA, 1999.
45. Kaloko, B.S.; Soebagio, M.H.P.; Purnomo, M.H. Design and development of small electric vehicle using MATLAB/Simulink. *Int. J. Comput. Appl.* **2011**, *24*, 19–23. [[CrossRef](#)]

46. Bampoulas, A.; Giannakis, A.; Tsaklidou, S.; Karlis, A. Modeling, simulation and performance evaluation of a low-speed battery electric vehicle. In Proceedings of the 2016 Eleventh International Conference on Ecological Vehicles and Renewable Energies (EVER), Monte Carlo, Monaco, 6–8 April 2016; IEEE: Piscataway, NJ, USA, 2016; pp. 1–8.
47. Mahmud, K.; Town, G.E. A review of computer tools for modeling electric vehicle energy requirements and their impact on power distribution networks. *Appl. Energy* **2016**, *172*, 337–359. [[CrossRef](#)]
48. Wai, C.K.; Rong, Y.Y.; Morris, S. Simulation of a distance estimator for battery electric vehicle. *Alex. Eng. J.* **2015**, *54*, 359–371. [[CrossRef](#)]
49. Larminie, J.; Lowry, J. *Electric Vehicle Technology Explained*; John Wiley & Sons: Hoboken, NJ, USA, 2012.
50. Ehsani, M.; Gao, Y.; Longo, S.; Ebrahimi, K. *Modern Electric, Hybrid Electric, and Fuel Cell Vehicles*; CRC Press: Boca Raton, FL, USA, 2018.
51. Sadeq, T.; Wai, C.K.; Morris, E. Current Control of Battery-Supercapacitors System for Electric Vehicles based on Rule-Base Linear Quadratic Regulator. *Adv. Sci. Technol. Eng. Syst. J.* **2021**, *6*, 57–65. [[CrossRef](#)]
52. Armenta-Déu, C. Battery Management for Improved Performance in Hybrid Electric Vehicles. *Vehicles* **2024**, *6*, 949–966. [[CrossRef](#)]
53. Sadeq, T.; Wai, C.K. Model the DC-DC converter with supercapacitor module based on system identification. In Proceedings of the 2019 IEEE International Conference on Automatic Control and Intelligent Systems (I2CACIS), Selangor, Malaysia, 29 June 2019; IEEE: Piscataway, NJ, USA, 2019; pp. 185–188.

Disclaimer/Publisher’s Note: The statements, opinions and data contained in all publications are solely those of the individual author(s) and contributor(s) and not of MDPI and/or the editor(s). MDPI and/or the editor(s) disclaim responsibility for any injury to people or property resulting from any ideas, methods, instructions or products referred to in the content.